Journal for ImmunoTherapy of Cancer

Bispecific binder redirected lentiviral vector enables in vivo engineering of CAR-T cells

Justin T Huckaby,[1] Elisa Landoni,[2] Timothy M Jacobs,[3] Barbara Savoldo,[2,4] Gianpietro Dotti,[2,5] Samuel K Lai [1,3,5]

To cite: Huckaby JT, Landoni E, Jacobs TM, *et al*. Bispecific binder redirected lentiviral vector enables in vivo engineering of CAR-T cells. *Journal for ImmunoTherapy of Cancer* 2021;**9**:e002737. doi:10.1136/jitc-2021-002737

► Additional supplemental material is published online only. To view, please visit the journal online (http://dx.doi.org/10.1136/jitc-2021-002737).

JTH and EL are joint first authors.

Accepted 18 June 2021

Check for updates

© Author(s) (or their employer(s)) 2021. Re-use permitted under CC BY-NC. No commercial re-use. See rights and permissions. Published by BMJ.

[1]UNC/NCSU Joint Department of Biomedical Engineering, UNC-Chapel Hill, Chapel Hill, North Carolina, USA
[2]Lineberger Comprehensive Cancer Center, UNC-Chapel Hill, Chapel Hill, North Carolina, USA
[3]Division of Pharmacoengineering and Molecular Pharmaceutics, UNC-Chapel Hill, Chapel Hill, North Carolina, USA
[4]Department of Pediatrics, UNC-Chapel Hill, Chapel Hill, North Carolina, USA
[5]Department of Microbiology and Immunology, UNC-Chapel Hill, Chapel Hill, North Carolina, USA

Correspondence to
Dr Samuel K Lai; lai@unc.edu

ABSTRACT

Background Chimeric antigen receptor (CAR) T cells have shown considerable promise as a personalized cellular immunotherapy against B cell malignancies. However, the complex and lengthy manufacturing processes involved in generating CAR T cell products ex vivo result in substantial production time delays and high costs. Furthermore, ex vivo expansion of T cells promotes cell differentiation that reduces their in vivo replicative capacity and longevity.

Methods Here, to overcome these limitations, CAR-T cells are engineered directly in vivo by administering a lentivirus expressing a mutant Sindbis envelope, coupled with a bispecific antibody binder that redirects the virus to $CD3^+$ human T cells.

Results This redirected lentiviral system offers exceptional specificity and efficiency; a single dose of the virus delivered to immunodeficient mice engrafted with human peripheral blood mononuclear cells generates CD19-specific CAR-T cells that markedly control the growth of an aggressive pre-established xenograft B cell tumor.

Conclusions These findings underscore in vivo engineering of CAR-T cells as a promising approach for personalized cancer immunotherapy.

BACKGROUND

Adoptive transfer of CD19-specific chimeric antigen receptor (CAR)-T cells has demonstrated considerable success for the treatment of B cell malignancies in patients with relapsed or refractory diseases,[1 2] providing the basis for at least three cell therapies (Yescarta for non-Hodgkin's lymphoma, Kymriah for acute lymphoblastic leukemia, and Tecartus for mantel cell lymphoma) approved by the US Food and Drug Administration (FDA) to date.[3] However, the generation of CAR-T cell products in all instances involves time consuming and complex manufacturing processes that delay the immediate availability of these cellular therapies for patients with aggressive disease and also lead to exorbitant costs.[4–8] Furthermore, activation, genetic manipulation, and ex vivo expansion of CAR-T cells inevitably leads to significant differentiation of T cells, which likely reduce their self-renewal capacity on adoptive transfer back into patients and consequently limiting the overall efficacy.[9–15]

Direct in vivo engineering of CAR-T cells, based on transducing T cells circulating in the peripheral blood with viral vectors, offers the potential to bypass the need for ex vivo manufacturing of patient-derived T cells entirely. Such viral vectors can serve as an off-the-shelf therapy immediately available to be infused in patients with aggressive disease, greatly expediting the therapy and markedly reducing the costs. Lentiviral (LV) vectors are already used to engineer CAR-T cells ex vivo in FDA-approved products, underscoring their ability to safely integrate the CAR transgene.[3 16 17] Unfortunately, conventional LV vectors, such as those pseudotyped with VSV-G, exhibit extremely broad tropisms; the lack of cell target specificity prohibits their direct use in vivo to target T cells.[18–20] Considerable efforts over the past two decades have led to engineering novel envelope glycoprotein pseudotypes, thereby establishing next-generation LVs retargeted to specific cell types via receptor binding.[21] To date, the most successful strategies involve several common features: (1) ablation of wildtype cell surface receptor binding, (2) display of an additional targeting domain for binding a new cell type either covalently or non-covalently, and (3) preservation of membrane fusion activity for entry into cells.[22]

Paramyxovirus and alphavirus glycoproteins have received the most attention for retargeting LVs given their completely separate protein domains for receptor binding and membrane fusion. Buchholz and colleagues have pioneered much of the paramyxovirus glycoprotein engineering work using measles virus and Nipah virus as their preferred pseudotypes.[22] Beginning with measles virus glycoproteins, the Buchholz team developed truncated versions of the hemagglutinin and

J Immunother Cancer: first published as 10.1136/jitc-2021-002737 on 12 September 2021. Downloaded from http://jitc.bmj.com/ on April 18, 2024 by guest. Protected by copyright.

fusion proteins that could effectively pseudotype LVs while codisplaying a covalently attached targeting ligand on the C-terminus of hemagglutinin.[23] Specific mutations were also applied to reduce native measles virus receptor tropism, enabling an efficient LV system for transducing unstimulated T lymphocytes directly in vivo.[24 25] More recently, Buchholz and colleagues applied a similar approach to Nipah virus glycoproteins, whereby a set of mutations was discovered to diminish native receptor binding and a specific site was established for adding surface exposed targeting ligands, such as single-chain antibodies or DARPins, for retargeting Nipah pseudotyped LVs to specific cell types.[26] Using their Nipah LVs retargeted to CD3, CD4, and CD8, they have been the only group to date to generate functional CAR-T cells directly in vivo for cancer immunotherapy by viral vector delivery.[22 27–31]

Chen and Wang pioneered much of the early alphavirus pseudotype development for LVs using mutant and novel versions of Sindbis virus glycoproteins. Chen and colleagues developed novel Sindbis E2 glycoprotein domains, responsible for receptor binding, by applying site-specific mutations to ablate native receptor tropism and direct addition of adapter binding molecules, such as the ZZ domain of protein A, avidin, biotin-adaptor peptide, and integrin-targeting peptide.[32–39] By mixing together LV and targeting ligand containing the adapter binding pair, such as Fc of antibody for ZZ domain, Sindbis-based LV could be redirected to a variety of receptors and cell types. A more recent extension of this strategy with Sindbis E2 was demonstrated using SpyTag and a disulfide bond-forming pair as adapter binding molecules for more permanent covalent incorporation of targeting ligand on viral surface.[40 41] Wang and colleagues adopted a similar strategy with an HA tag in their E2 domain or direct coexpression of full IgG antibody molecules on viral surface while focusing much of their efforts on engineering enhanced Sindbis E1 fusogen variants.[42–46] Although these various groups have demonstrated significant enhancement in transduction of immune and tumor cell types both in vitro and in vivo with their Sindbis pseudotyped LV systems, no one has yet to test the ability of a Sindbis LV system to transduce circulating primary T cells or generate CAR-T cells directly in vivo for cancer immunotherapy.

The current lengthy manufacturing processes to generate CAR-T cell products and increasing development of targeted gene delivery viral vectors motivated us to develop a LV-based gene transfer system with considerable specificity and efficiency for T cell targeting in vivo. To minimize transduction of non-target cells, we incorporated a mutated Sindbis pseudotyped lentiviral vector (SINV-LV), with mutations to the E2 glycoprotein that abrogate its native tropism to human cells (online supplemental figure S1A). To redirect the mutant SINV-LV to T cells, which lacks, any specific cell tropism or additional adapter molecule residues in the E2 receptor binding domain, we engineered a separate bispecific binder that can bind: (1) the mutant E2 glycoprotein on SINV-LV and (2) CD3, a ubiquitous coreceptor on all T cells (figure 1A). Our novel LV system thus comprises simply mixing SINV-LV with bispecific binders for non-covalent attachment and redirection to target T cells in vivo.

METHODS

Cell lines and primary cells

B cell lymphoma tumor cell lines (BV-173 and Daudi) and T cell lymphoma tumor cells (Sup-T1) were purchased from ATCC and cultured in RPMI-1640 medium (Gibco) supplemented with 10% HyClone FBS (GE Healthcare), penicillin (100 U/mL; Gibco), and streptomycin (100 U/mL; Gibco). All cells were maintained at 37 °C and 5% CO_2 for growth. All cell lines are regularly tested for Mycoplasma, and the identity of each cell line was validated via flow cytometry for relevant surface markers and also monitored for morphological drift in culture. Cell lines were maintained in culture no longer than 30 days and then replaced with an earlier passage of cells thawed from cryopreservation. BV-173 cells were transduced with a gamma retroviral vector encoding the Firefly-Luciferase (FFluc) gene. Sup-T1 cells ($CD3^+TCR^-$) were engineered with the TCR specific for $Tyrosinase_{368\text{-}376}$ (obtained from Frankel and colleagues)[47] in order for Sup-T1 cells to express endogenous CD3 on the cell surface.[48 49] Peripheral blood mononuclear cells (PBMCs) were isolated from fresh buffy coats (Gulf Coast Regional Blood Center) using Lymphoprep medium (Accurate Chemical and Scientific Corporation). PBMCs were then activated for 48 hours in bioreactors with soluble anti-CD3 (200 ng/mL; Miltenyi Biotec) and anti-CD28 (200 ng/mL; BD Biosciences) mAbs. Activated PBMCs were washed with PBS and allowed to rest at 37°C and 5% CO_2 in growth culture medium for at least 24 hours prior to LV transduction or in vivo studies. Primary T cells were activated, cultured, and transduced in complete medium consisting of 45% Click's Medium (Irvine Scientific), 45% RPMI-1640 (Gibco), 10% HyClone FBS (GE Healthcare), 2 mmol/L GlutaMax (Gibco), penicillin (100 U/mL; Gibco), and streptomycin (100 U/mL; Gibco) with 10 ng/mL IL-7 and 5 ng/mL IL-15 (PeproTech).

In vitro transduction assays

The $CD3^+$ Sup-T1 tumor cell line was transduced with SINV-GFP in the presence of increasing concentrations of tFab to demonstrate BsAb-mediated enhanced transduction of target cells. Sup-T1 cells were seeded in sterile 96-well tissue culture treated plates (Corning Costar Cat # 3599) at 1×10^5 cells/well. SINV-GFP at a multiplicity of infection (MOI) of 25, based on qPCR titering, was premixed with various concentrations of tFab in serum-containing growth culture medium for 1 hour at room temperature to allow tFab to bind onto the surface of SINV-GFP particles before directly adding this transduction mixture to the plated cells. Each tFab concentration tested (1, 10, 30, and 50 nM) is reported as the

J Immunother Cancer: first published as 10.1136/jitc-2021-002737 on 12 September 2021. Downloaded from http://jitc.bmj.com/ on April 18, 2024 by guest. Protected by copyright.

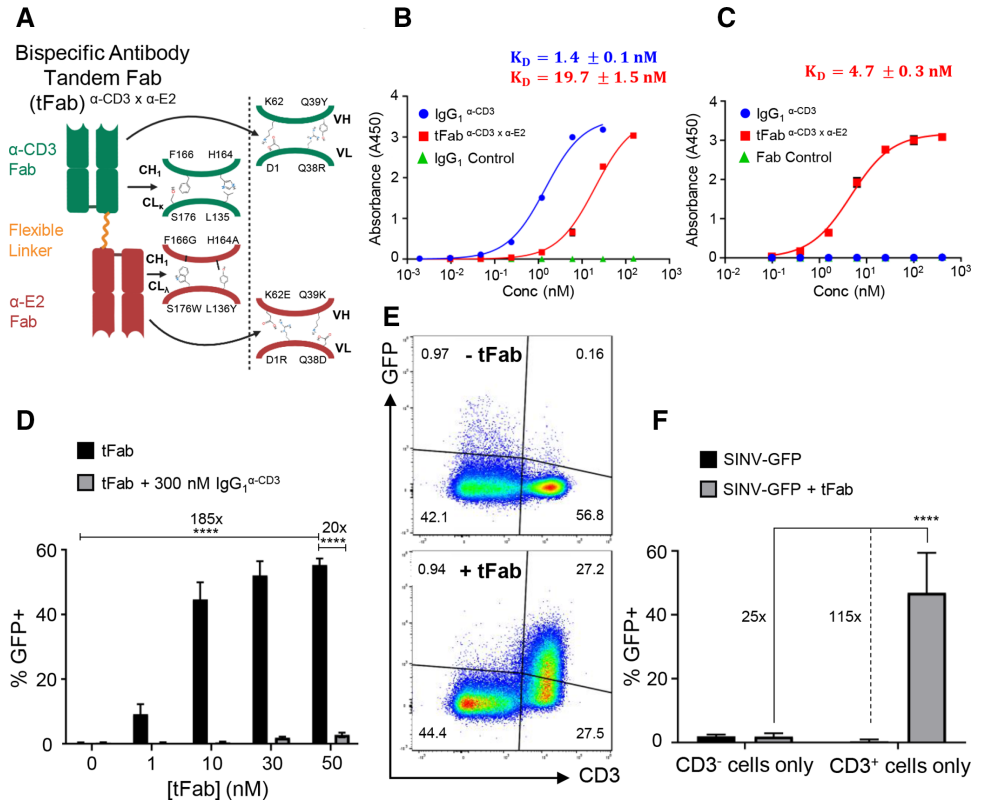

Figure 1 Bispecific antibody binder enhances specificity and transduction efficiency of the mutant lentivirus. (A) Schematic of bispecific antibody in tandem Fab format (tFab) used for redirecting mutant Sindbis lentiviral vector (SINV-LV) to CD3$^+$ T cells for targeted transduction. Orthogonal amino acid mutation sets are shown for constant and variable domains of each Fab to ensure correct pairing of heavy and light chains. (B) Binding affinity of control IgG (blue) and tFab (red) to human CD3ε analyzed by ELISA (n=2). (C) Binding affinity of tFab (red) to mutant Sindbis E2 glycoprotein analyzed by ELISA (n=2). (D) SINV-GFP transduction to CD3$^+$ T cells is enhanced by addition of the tFab molecule in a concentration-dependent manner. At all tested concentrations, excess anti-CD3 IgG of the same clone blocked tFab-mediated SINV-GFP transduction, suggesting that transduction was specifically mediated via tFab binding CD3 in T cells. Data represent results of three independent experiments performed in triplicate (MOI=25) and analyzed using a two-way ANOVA with a post hoc Tukey's test for multiple comparisons (****p<0.0001). (E) addition of tFab to mutated Sindbis pseudotyped lentiviral vector encoding green fluorescent protein (SINV-GFP) redirects the mutant lentiviral vector to CD3$^+$ T cells in a mixed culture (CD3$^+$ and CD3$^-$ cells together) demonstrating the specificity towards CD3$^+$ T cells. (F) in mixed cultures of CD3$^+$ (Sup-T1) and CD3$^-$ (BV-173) cells, SINV-GFP plus tFab demonstrated substantial selectivity towards CD3$^+$ T cells as indicated by the increase in percentage of GFP$^+$ cells. data represent results of three independent experiments performed in triplicate (MOI=25; (tFab)=30 nM) and analyzed using a two-way ANOVA with a post hoc Tukey's test for multiple comparisons (****p<0.0001). ANOVA, analysis of variance; MOI, multiplicity of infection.

final concentration of the tFab once diluted and added to cells for transduction in 96-well plates. To confirm enhanced transduction was dependent on the CD3 specificity of the tFab, excess $IgG_1^{\alpha\text{-}CD3}$ (300 nM) was added to replicate sample wells at each tFab concentration to competitively block binding of CD3 as entry receptor for targeted transduction with SINV-GFP plus tFab. After 24 hours of transduction at 37 °C and 5% CO_2, cells were washed twice with cold growth culture medium using low-speed plate centrifugation (300× g) to remove residual antibody and LV prior to resuspension in fresh growth culture medium. Cells were allowed to grow and express GFP transgene for 72 hours at 37 °C and 5% CO_2 prior to washing them into PBS and analyzing their GFP expression via flow cytometry using an Attune NxT flow cytometer with plate autosampler (Applied Biosystems).

A similar transduction assay with CD3 + Sup-T1 and CD3– BV-173 tumor cell lines was established to demonstrate specificity and selectivity of SINV-GFP plus tFab transduction to CD3$^+$ target cells. Sup-T1 and BV-173 cells were seeded together at a 1:1 ratio in each well of sterile 96-well tissue culture treated plates (Corning Costar Cat # 3599) at 1×10^5 total cells/well. SINV-GFP at a MOI of 25, based on qPCR titering, was premixed with 30 nM final concentration of tFab in serum-containing growth culture medium for 1 hour at room temperature before directly adding this transduction mixture to the plated co-culturing cells. A control transduction of SINV-GFP at MOI 25 without addition of tFab was also dosed to co-culturing cells. After 24 hours of transduction at 37 °C and 5% CO_2, cells were washed twice with cold growth culture medium using low-speed plate centrifugation (300× g) to

J Immunother Cancer: first published as 10.1136/jitc-2021-002737 on 12 September 2021. Downloaded from http://jitc.bmj.com/ on April 18, 2024 by guest. Protected by copyright.

remove residual antibody and LV prior to resuspension in fresh growth culture medium. Cells were allowed to grow and express GFP transgene for 72 hours at 37 °C and 5% CO_2 prior to washing them into PBS for surface marker phenotype staining with anti-CD3 APC (BD Cat # 340440) and anti-CD19 PE (BD Cat # 340364). Phenotypic antibody staining was allowed to proceed for 30 min at 4°C followed by two PBS washes of samples to remove unbound antibodies. Washed cells were resuspended into PBS and analyzed for their GFP expression via flow cytometry using an Attune NxT flow cytometer with plate autosampler (Applied Biosystems).

Activated primary human PBMCs were transduced with SINV-CAR at a MOI of 10, based on qPCR for vector titer and total number of PBMCs, with and without addition of tFab to demonstrate functional CAR expression and subsequent cytotoxic activity of CAR-T cells in vitro. In brief, 2.5×10^5 activated PBMCs were transduced in 250 µL final volume per well of growth culture medium supplemented with IL-7 and IL-15 cytokines in 48-well tissue culture treated plates. SINV-CAR at a MOI of 10 (ie, 2.5×10^6 infectious units (IUs) based on qPCR titering) was premixed with 50 nM final concentration of tFab in serum-containing growth culture medium for 1 hour at room temperature before directly adding this transduction mixture to the plated PBMCs. SINV-CAR at MOI 10 was also dosed directly without addition of tFab for targeting along with other non-transduced control PBMC sample wells. After 6 hours of transduction at 37 °C and 5% CO_2, PBMC samples were washed twice with cold growth culture medium to remove residual antibody and LV prior to resuspension in fresh growth culture medium and transfer to a new, sterile 24-well tissue culture treated plate for 84 hours of growth and CAR expression at 37 °C and 5% CO_2. A portion of each sample well was collected and washed into PBS for phenotypic surface marker staining by a panel of antibodies and subsequent CAR expression analysis using an LSR Fortessa flow cytometer (BD Biosciences). The remaining PBMCs in each sample well were resuspended and counted by trypan blue dye exclusion for subsequent plating with $CD19^+$ tumor B cells to demonstrate CAR functionality by a coculture cytotoxicity assay described in more details below.

In vitro coculture tumor cytotoxicity assay

Transduced and non-transduced control PBMCs (1.5×10^5 cells/well or 3×10^5 cells/well) were cocultured with tumor cell lines (BV-173 or Daudi, 1.5×10^5 cells/well in 24-well plates), in complete medium, in the absence of cytokines (E:T=1:1 or E:T=2:1). The effector-to-target (E:T) ratio was not normalized to CAR + transduced T cells but was instead based on the total number of T cells in culture, including both transduced and non-transduced fractions taken together without separation. After 4–5 days of culture, cells were harvested and stained with CD3 (APC-H7, clone SK7 from BD Biosciences) and CD19 (FITC, clone SJ25C1 from BD Biosciences) monoclonal Abs to detect T cells and tumor cells, respectively. Residual tumor cells in culture were enumerated by flow cytometry. Culture supernatants were harvested after 24 or 48 hours of culture and IFN-γ and IL-2 measured using the DuoSet Human IFN-γ and DuoSet Human IL-2 ELISA kits respectively (R&D Systems). Data acquisition was performed on a Synergy2 microplate reader (BioTek) using the Gen5 software.

Tumor mouse model for testing efficacy of in vivo generated CAR-T cells

Female NSG mice (7–9 weeks of age, obtained from the University of North Carolina Animal Services Core) were used to establish our chronic myeloid leukemia xenograft tumor mouse model. Mice were irradiated at a low dose (100 rad) by a cesium irradiator on day −6 of the study prior to any cell engraftments. The following day (day −5), 5×10^5 FFLuc BV-173 tumor B cells were injected in 150 µL sterile PBS via intravenous tail vein. After allowing 5 days for tumor cell engraftment, 5×10^6 activated PBMCs were injected on day 0 in 150 µL sterile PBS via intravenous tail vein. Thirty min after infusing the PBMCs, mice were randomly separated into two different treatment groups: (1) SINV-CAR without tFab or (2) SINV-CAR with premixed tFab. In both groups, SINV-CAR was dosed at 2.5×10^7 IUs, based on qPCR, in 150 µL sterile PBS per mouse via intravenous tail vein injection. This dosage equated to 5×10^{10} viral particles per mouse, based on absolute particle counts of SINV-CAR using NanoSight NS500 (Malvern Panalytical) nanoparticle tracking analysis. tFab (5 µg/mouse) was premixed with SINV-CAR for 1 hour at room temperature in 150 µL sterile PBS prior to intravenous injections. B cell tumor growth was monitored weekly by bioluminescent imaging (BLI; total flux, photons/s) using an Ami HT optical imaging system (Spectral Instruments Imaging). Peripheral blood samples were taken weekly from mice via the submandibular route. Peripheral blood was subjected to red blood cell lysis followed by antibody staining and flow cytometry to assess number of human T cells ($CD3^+$) and tumor B cells ($CD19^+$) in circulation. Mice were sacrificed according to UNC guidelines for either tumor growth or occurrence of signs of discomfort, such as tumor-mediated paralysis. On sacrifice, peripheral blood was collected from cardiac puncture of the heart, and spleens were measured and weighed prior to smashing over cell strainers into single cell suspensions. Blood and spleen were subjected to red blood cell lysis, antibody staining, and flow cytometry using an LSR Fortessa flow cytometer (BD Biosciences) to detect and quantify CAR^+ T cells and $CD19^+$ tumor B cells in isolated tissues. Antibodies used for phenotypic staining of in vivo samples included CD3 (APC-H7, clone SK7), CD8 (Alexa Fluor 700, clone RPA-T8), CD45 (APC, clone 2D1) and CD19 (FITC, clone SJ25C1) along with CountBright absolute counting beads (Invitrogen). All flow cytometry data analysis was performed with FlowJo V.10 software.

Statistical analysis

All data are presented as mean±SD. GraphPad Prism V.8 software was used to generate graphs and perform

J Immunother Cancer: first published as 10.1136/jitc-2021-002737 on 12 September 2021. Downloaded from http://jitc.bmj.com/ on April 18, 2024 by guest. Protected by copyright.

statistical analyses. Either Student's t-test or two-way analysis of variance (ANOVA) was used to determine statistically significant differences between treatment groups. Either a post hoc Tukey's test or Bonferroni correction was performed to correct for multiple comparisons after two-way ANOVA. Survival analysis was performed using the Kaplan-Meier method with a log-rank test to determine statistical significance. All p values less than 0.05 were considered statistically significant.

RESULTS

As proof of concept, we engineered bispecific binders in a tandem Fab format (tFab), comprised of two distinct Fab domains linked via a glycine-serine flexible linker and lacking the Fc antibody domain (figure 1A; online supplemental figure S1B). By applying different sets of orthogonal amino acid mutations[50] to the two Fab domains (anti-CD3 and anti-E2), we were able to overcome traditional heavy/light chain mispairing[51] and produce a pure population of bispecific tFab binders with properly paired Fabs by simple immobilized metal affinity chromatography purification (online supplemental figure S1C). We performed several immunoassays, including ELISAs (figure 1B,C), dot blots (online supplemental figure S1D), and immunogold labeling with transmission electron microscopy (online supplemental figure S1E), to characterize the specificity and affinity of the tFab binding to both human CD3ε and mutant Sindbis E2 glycoprotein. The tFab bound to both CD3ε and E2 at low nanomolar affinities (K_D=19.7 nM and 4.7 nM, respectively) as assessed by ELISA, whereas control anti-CD3 IgG of the same Fab clone ($IgG_1^{\alpha\text{-}CD3}$) bound only to CD3ε. Anti-CD3 IgG possessed higher binding affinity (K_D=1.4 nM), which is likely a direct consequence of the dimeric nature of two Fabs per IgG molecule. Using different lentivirus pseudotypes including SINV, VSV-G, and measles virus in dot blot experiments, we confirmed tFab binds specifically to only SINV-LV.

To evaluate the capacity of the SINV/tFab platform in targeting human T cells, we generated SINV-LV encoding an eGFP fluorescent reporter transgene (denoted as SINV-GFP), mixed with different amounts of tFab, and quantified the level of induced eGFP expression in a $CD3^+$ human cell line (Sup-T1). We found a tFab dose-dependent transduction enhancement that saturated at ~50 nM concentration of tFab (figure 1D). Without addition of the tFab, the transduction efficiency of SINV-GFP alone was less than 1%, whereas 50 nM of tFab enabled transduction of >50% of the cells. The increased transduction was a direct consequence of the combination of SINV-GFP and tFab redirection, as demonstrated by competitive inhibition in the presence of excess amounts of anti-CD3 IgG_1 (300 nM) (figure 1D). To further validate the specificity of viral targeting, we tested SINV-GFP/tFab in coculture experiments mixing $CD3^+$ (Sup-T1) and $CD3^-$ (BV-173) cells. As expected, without addition of the tFab, SINV-GFP showed negligible transduction of either $CD3^+$ or $CD3^-$ cells (figure 1E). In contrast, SINV-GFP/tFab showed a ~25 fold enhanced transduction of $CD3^+$ versus $CD3^-$ cells (figure 1F). This is consistent with previous work from our group comparing the transduction efficiency of wildtype versus mutant SINV-GFP in the presence or absence of tFab against tumor cell lines in vitro, where we found mutations to the Sindbis glycoprotein significantly reduced non-specific, background transduction, while addition of tFab restored efficient transduction, presumably by enhancing binding and internalization via receptor-specific interactions.[52]

We next cloned a second-generation CD19-specific CAR encoding the CD28 costimulatory endodomain into our SINV-LV (SINV-CAR; figure 2A) and tested the transduction efficiency in primary human T cells. At relatively moderate multiplicities of infection (MOI=10) without spinoculation or transduction enhancers, the SINV-CAR/tFab yielded ~1.2%–2.5% CAR-T cells, including both $CD4^+$ and $CD8^+$ cells, which was ~2 fold higher fraction than the SINV-CAR alone (p=0.0437; figure 2B; online supplemental figure S2C). To determine if CAR-T cells were functionally active, we developed an in vitro coculture assay to measure CAR-T cell cytotoxicity and cytokine secretion in presence of $CD19^+$ tumor cells (BV-173) (figure 2C). Even at very low effector-to-target (E:T) cell ratios (~1–5 CAR^+ T cells per 100 tumor cells; see Methods section for description of calculations), CAR-T cells generated from SINV-CAR/tFab eliminated far more (up to ~6 fold) tumor cells within 4 days than CAR-T cells generated from SINV-CAR alone (figure 2D; online supplemental figure S2D). A similar trend was observed using another $CD19^+$ tumor cell line (Daudi). The observed cytotoxic effect was consistent with the detection of IFN-γ and IL-2 in the culture medium collected within 24–48 hours of coculturing (figure 2E; online supplemental figure S2E). Although we noticed that the production of IFN-γ and IL-2 from CAR-T cells was higher when cocultured with the Daudi cell line, this is likely due to the expression of costimulatory markers (CD80 and CD86) from Daudi, which are not present in the BV-173 cell line (online supplemental figure S2F).

Based on these findings, we next evaluated the efficacy of the SINV-CAR/tFab vector system in a xenograft mouse model (figure 3A). $CD19^+$ BV-173 cells, engineered to express firefly luciferase as imaging reporter to allow monitoring of tumor growth in vivo, were engrafted into NSG mice. Five days later, activated human PBMCs were injected intravenously into the animals, followed by SINV-CAR with or without tFab 30 min later. By day 24, following SINV-CAR injection, mice treated with SINV-CAR/tFab displayed significantly reduced tumor bioluminescence (BLI) compared with control mice infused with SINV-CAR alone (figure 3B,C; online supplemental figure S3A). Control mice began developing hind-limb paralysis due to tumor localization in the spine, which necessitated sacrificing all animals at a much earlier time point (10 days earlier according to median survival times) than mice treated with SINV-CAR/tFab

J Immunother Cancer: first published as 10.1136/jitc-2021-002737 on 12 September 2021. Downloaded from http://jitc.bmj.com/ on April 18, 2024 by guest. Protected by copyright.

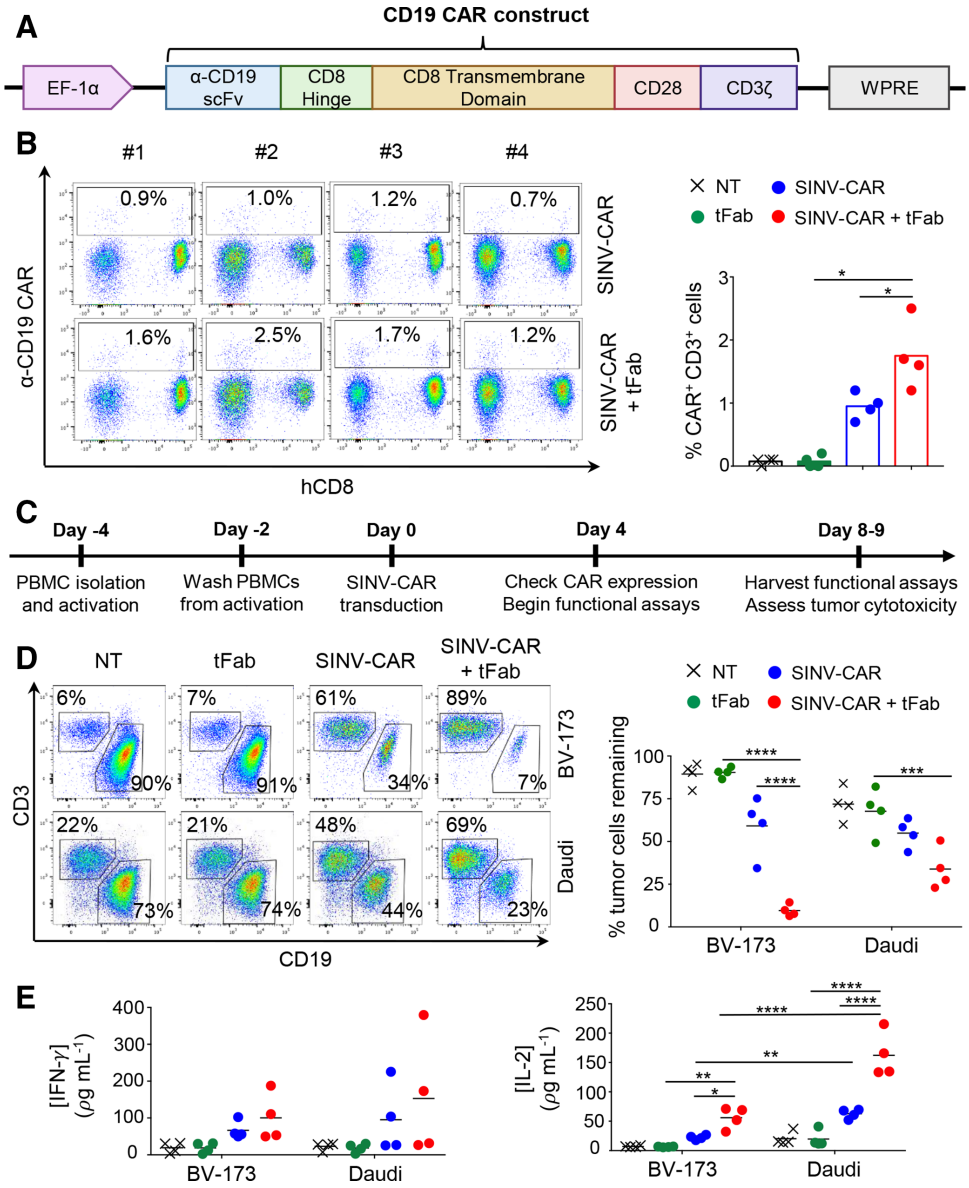

Figure 2 T cells transduced with SINV-CAR in combination with tFab express functional CD19.CAR and eliminate tumor B cells in vitro. (A) Schematic representation of the CD19.CAR cassette under the control of the EF-1α promoter and WPRE post-transcriptional regulatory molecule. (B) Flow cytometry plots (left) and summary (right) showing CAR expression in T cells transduced with SINV-CAR or SINV-CAR plus tFab. Non-transduced (NT) and tFab alone samples of T cells are provided as negative controls (n=4, mean shown). *P=0.0437 SINV-CAR plus tFab versus SINV-CAR; *p=0.0100 SINV-CAR plus tFab versus tFab with paired t-test. (C) Experimental schema for the transduction and subsequent coculturing of CAR-T cells with tumor B cells in vitro. (D) Representative flow plots (left panel) and summary (right panel) of the quantification of residual $CD19^+$ tumor B cells (BV-173 and Daudi cell lines) remaining after coculturing with either NT, tFab, SINV-CAR, or SINV-CAR plus tFab treated T cells (E:T=2:1). All cells were collected after 4 or 5 days (BV-173 and Daudi, respectively) and stained with CD3 and CD19 mAbs to identify T cells and tumor cells, respectively, by flow cytometry (n=4, mean shown). ***P=0.0004, ****p<0.0001, two-way ANOVA. (E) Quantification of IFN (left panel) and IL-2 (right panel) cytokines in supernatant collected after 24 hours of coculturing NT, tFab, SINV-CAR, or SINV-CAR plus tFab treated T cells with tumor cell lines (E:T=2:1) (n=4, mean shown). *P=0.0393, **p<0.0087, ****p<0.0001, two-way ANOVA. ANOVA, analysis of variance; CAR, chimeric antigen receptor; tFab, tandem Fab format.

(figure 3D). We attempted to quantify CAR^+ and $CD3^+$ human T cells circulating in the peripheral blood. While only very small numbers of CAR^+ and $CD3^+$ human T cells were detected at early time points (online supplemental figure S3B,C), we found a substantial quantity of CAR^+CD3^+ human T cells in the peripheral blood of all mice treated with SINV-CAR/tFab at the time of sacrifice, while the $CD3^-$ cells did not express the CAR (figure 3E; online supplemental figure S3D). These greater levels of CAR^+CD3^+ human T cells were attributed to greater T cell transduction by SINV-CAR/tFab versus SINV-CAR and not attributed to simply greater total number of T cells in the peripheral blood, as total T cell counts were

J Immunother Cancer: first published as 10.1136/jitc-2021-002737 on 12 September 2021. Downloaded from http://jitc.bmj.com/ on April 18, 2024 by guest. Protected by copyright.

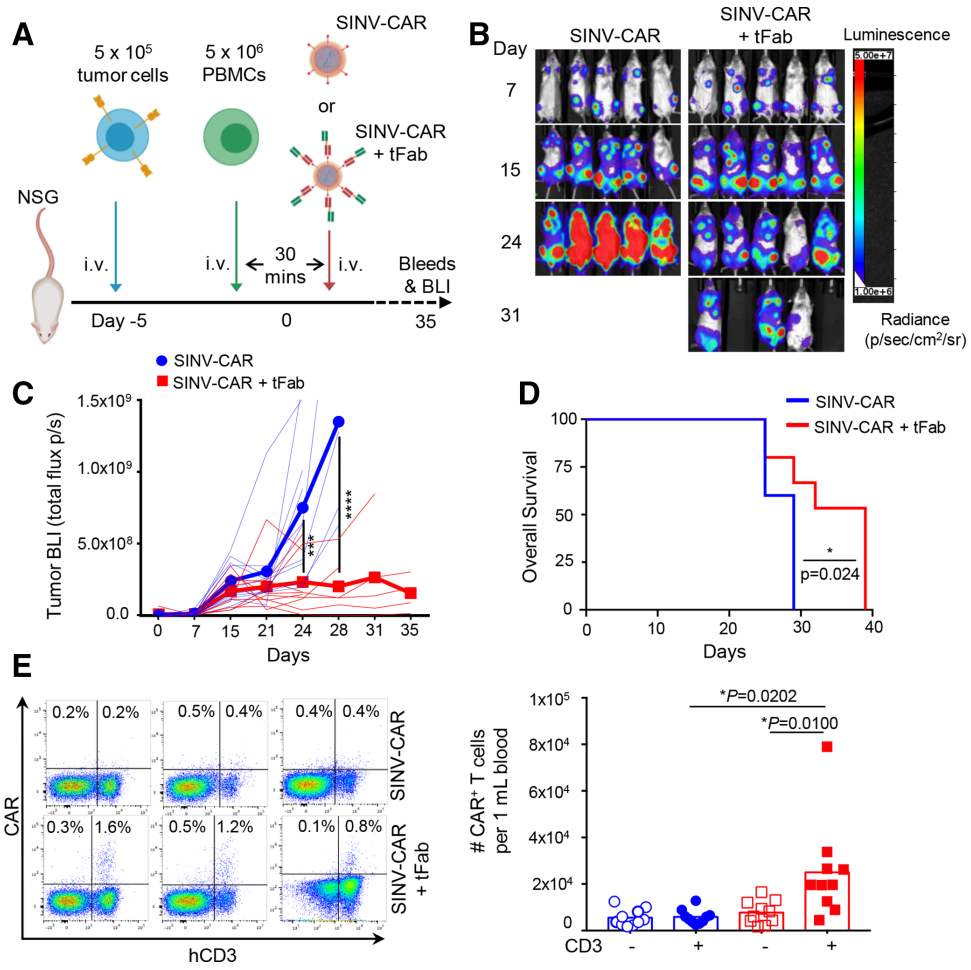

Figure 3 SINV-CAR targeted with tFab generates functional CAR-T cells directly in vivo. (A) Experimental schema of the mouse model. Following a lose dose of irradiation (100 rad), mice were injected with FFLuc BV-173 (5×10^5 cells) intravenously. Five days later, mice were injected intravenously with 5×10^6 activated PBMCs followed by either SINV-CAR alone or SINV-CAR plus tFab 30 min later. (B) Representative tumor bioluminescence (BLI) (color scale: min=1×10^6; max=5×10^7) for mice treated according to scheme from panel A. (C) BLI kinetics for all mice treated according to scheme from panel A. Lighter lines represent individual mice, while bolded lines represent the means for the treatment groups. Summary of two independent experiments (n=10 mice for each condition). ***P=0.0002; ****p<0.0001, two-way ANOVA with Bonferroni correction. (D) Kaplan-Meier survival curve for all mice (n=10 mice per condition) treated according to scheme from panel A. *P=0.0242, log-rank test. (E) Representative flow plots (left panel) and quantification (right panel) of CAR-T cells in the $CD3^-$ (open symbols) and $CD3^+$ (filled symbols) populations (gated on live cells) in the peripheral blood at the time of euthanasia (n=10 each condition, mean shown). *P=0.0100 and *p=0.0202, unpaired t-test. ANOVA, analysis of variance; CAR, chimeric antigen receptor; PBMCs, peripheral blood mononuclear cells.

similar between both treatment groups (online supplemental figure S3E).

The aggressive BV-173 B cell lymphoma model appears to result in accumulation and spread of tumor cells in the spleen: at the time of sacrifice, we discovered very enlarged spleens in mice treated with SINV-CAR alone (figure 4A; online supplemental figure S4A), with a very high proportion of BV-173 tumor cells in the enlarged spleens (>50% of the total cell populations on average) (figure 4B). In contrast, the overall size and weight of spleens from mice treated with SINV-CAR/tFab appeared comparable with those from normal, healthy mice. Analysis of the cellular composition of the spleens revealed higher infiltration of CAR-T cells in mice treated with SINV-CAR/tFab (figure 4C; online supplemental figure S4C,D), which correlated with much lower numbers of $CD19^+$ BV-173 tumor cells (<1% on average) (figure 4B). Taken together, these data suggest that generating even a relatively small number of CAR-T cells directly in vivo is sufficient to enable tumor suppression in lymphoid organs and significantly prolong the median survival time of tumor-bearing mice.

CONCLUSION

In conclusion, we have developed a modular gene delivery platform, using a mutant Sindbis LV vector redirected to target cells via bispecific tFab binders. This LV platform enabled highly specific and effective gene delivery to target cells in vivo even at modest

J Immunother Cancer: first published as 10.1136/jitc-2021-002737 on 12 September 2021. Downloaded from http://jitc.bmj.com/ on April 18, 2024 by guest. Protected by copyright.

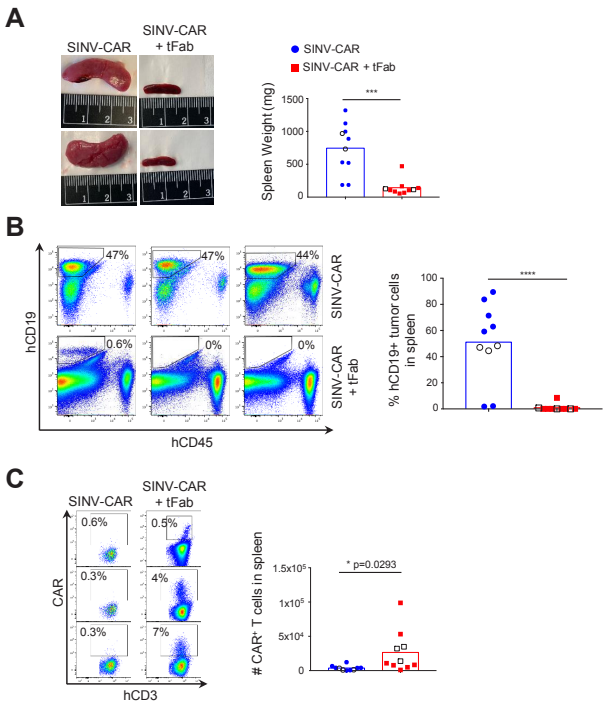

Figure 4 SINV-CAR targeted with tFab suppresses tumor growth in spleen. (A) Mice engrafted with FFLuc BV-173 tumor cells and treated with either SINV-CAR alone or SINV-CAR plus tFab were euthanized, and spleens were weighed (right, n=10, mean shown). Representative images of the spleens (left panel). ***P=0.0002, unpaired t-test. (B) Representative flow plots (left panel) and summary (right panel) of the percentage of human CD19$^+$ tumor B cells infiltrating the spleen of mice engrafted with FFLuc BV-173 and treated with either SINV-CAR alone or SINV-CAR plus tFab at time of sacrifice (n=10, mean shown). ****P<0.0001, unpaired t-test. (C) Representative flow plots (left panel) and quantification (right panel) of human CAR-T cells (gated on CD3$^+$CD45$^+$) in the spleen at the time of euthanasia (n=10 each condition, mean shown). Empty symbols denote the flow plots shown to the left. *P=0.0293, unpaired t-test. CAR, chimeric antigen receptor; tFab, tandem Fab format.

MOIs. Compared with recent studies of in vivo generated CAR-T cells from the Buchholz team using Nipah pseudotyped LVs, we injected similar particle doses per mouse between our studies (5×10^{10} SINV-LV vs $1–2.5\times10^{11}$ Niv-LV).[28 30 31] Although particle titers were measured by the same method of nanoparticle tracking analysis using similar Nanosight instruments, Buchholz *et al*[21] established a different efficacy mouse model engrafting Nalm-6 tumor B cells, so a direct comparison of our in vivo results is not feasible. Similarly, direct comparisons of transduction efficiency in vitro are difficult: we determine MOI based on a qPCR titer, which provide an absolute count of viruses carrying the transgene without inferring details on viral particle functionality or infectivity. In contrast, many groups report functional titers established from transduction assays on particular cell lines, which produce different titer values without specific details of viral transgene or particle content.[23 25 27 29 30 32 40 41 43–45 53]

Although retargeted measles and Nipah pseudotyped LVs seem to achieve significantly greater in vitro transduction rates compared with our SINV-LV/tFab in primary PBMCs, it is worth noting that our transduction protocol did not include spinoculation or enhancers such as Vectofusin-1.[23 27 29–31] Nevertheless, measles and Nipah pseudotyped LVs retargeted to T cells were able to transduce unstimulated cells in vitro and in vivo, which we are currently unable to achieve with our SINV-LV/tFab. This difference might be explained by the divergent mechanisms used by alphaviruses and paramyxoviruses for infection: alphaviruses, such as Sindbis, require pH-dependent membrane fusion following endocytosis to deliver the cargo DNA, whereas paramyxoviruses, such as measles and Nipah, are pH independent and do not rely on endocytosis to deliver their cargo DNA into cells.[22]

The differences between Sindbis and other paramyxoviruses notwithstanding, we showed here that a single dose of our targeted Sindbis-based LV vector was able to generate CAR-T cells from circulating T lymphocytes in a humanized tumor mouse model of B cell leukemia. The in vivo engineered CAR-T cells from this proof-of-concept study greatly suppressed CD19$^+$ tumor cell growth and prolonged the overall survival time of mice, despite the highly aggressive nature of the tumor model. The efficient transduction was critically dependent on the bispecific tFab binders redirecting mutant Sindbis pseudotyped LVs to circulating T-lymphocytes. While the other previously discussed LV surface engineering approaches employ mutations and addition of either adapter molecules for non-covalent targeting or directly incorporated targeting ligands, our SINV-LV only requires mutations without the need for incorporating additional residues that might compromise particle integrity and titer. Our system does not require empirical testing of new targeting ligands swapped onto the particle surface as covalent attachments but only engineering of the bispecific binder molecule. Furthermore, antibody engineering with directed evolution will allow us to screen for a library of bispecific binder molecules enabling fully tunable affinity toward both LV surface glycoproteins and cell receptors. By exchanging our current anti-CD3 cell receptor binding Fab arm for specificity toward a different receptor, we could target CD4$^+$ or CD8$^+$ T cells without modifications to our LV vector, even enabling us to multiplex with trispecific binders for enhanced cell specificity. This modular nature provides numerous possibilities for a wide variety of cell and gene therapy applications beyond just CAR-T cell immunotherapy, but it would require separate development of both bispecific binder and LV vector if a different cell type were to be targeted with a different genetic cargo, such as a different CAR molecule or therapeutic transgene.

The antitumor activity that we observed in vivo, considering the low number of CAR-expressing T cells, is consistent with the superior performance and self-renewal capacity of CAR-T cells directly generated in vivo compared with that of CAR-T cells stimulated and expanded more

J Immunother Cancer: first published as 10.1136/jitc-2021-002737 on 12 September 2021. Downloaded from http://jitc.bmj.com/ on April 18, 2024 by guest. Protected by copyright.

extensively ex vivo. However, this theory has yet to be thoroughly explored by us or any other research group generating CAR-T cells directly in vivo. The only study to date to directly compare efficacy of in vivo versus ex vivo generated CAR-T cells was led by Matthias and colleagues, who utilized a non-viral polymeric nanoparticle platform for systemic delivery of anti-CD19 CAR to a fully mouse model of leukemia.[54] Their results suggest that CAR-T cells, whether engineered directly in vivo with their novel integrating nanoparticle platform or ex vivo from traditional LV transduction, could achieve similar levels of tumor remission and prolonged animal survival in a preclinical mouse model of leukemia. However, the comparison in this study was made from different gene delivery vectors at high doses for both nanoparticles (five sequential injections of 3×10^{11} particles) and ex vivo generated CAR-T cells (5 million CAR-T per mouse). Future studies comparing in vivo and ex vivo generated CAR-T cells should apply identical gene delivery vectors in both treatment groups and contextualize the efficacious dose range of ex vivo generated CAR-T cells by injecting at the lower dosage limit for therapy. Simultaneously, the dosage range of systemically delivered gene delivery vector should be optimized so as to correlate an in vivo vector dose with similar efficacy observed from a particular dosage of ex vivo generated CAR-T cells. Simply measuring the number of CAR^+ T cells generated in a tumor-bearing mouse model following different doses of gene vector may not represent the complex activity of CAR engagement and cell stimulation occurring in vivo upon tumor antigen recognition. As the new field of in vivo CAR-T engineering continues to develop, carefully designed studies comparing performance and relevant doses in context to more traditional ex vivo engineered CAR-T are imperative to understand the feasibility of this novel approach and essential in understanding the limitations that must be circumvented for such a therapy to reach the clinic.

Acknowledgements Animal studies were performed within the UNC Lineberger Animal Studies Core Facility at the University of North Carolina at Chapel Hill. The UNC Lineberger Animal Studies Core is supported in part by an NCI Center Core Support Grant (CA16086) to the UNC Lineberger Comprehensive Cancer Center. Special thanks is given to both the Biomedical Research Imaging Center (BRIC) and Flow Cytometry Core Facility at UNC for use of their instruments, which are supported in part by a Cancer Center Core Support Grant (P30 CA016086) to the UNC Lineberger Comprehensive Cancer Center. Transmission electron microscopy and grid preparation were performed by Paul Risteff at the UNC Hooker Imaging Core Facility. Special thanks to Boris Kantor and Logan Brown of the Duke University Viral Vector Core for their production of concentrated, in vivo grade lentiviruses used in these studies.

Contributors JTH and EL contributed equally to this work. All authors conceptualized the project framework and designed experiments. JTH and TMJ designed and developed the bispecific binder molecule and lentiviral vector. JTH performed in vitro transductions. EL isolated and cultured primary cells. JTH and EL conducted tumor coculture cytotoxicity studies. EL handled mice and performed bioluminescent imaging. JTH and EL processed mouse tissue samples and performed flow cytometry phenotypic analyses. JTH and EL analyzed the data and performed statistical analysis. All authors contributed in writing and editing the manuscript.

Funding This work was supported in part by the National Science Foundation Graduate Research Fellowship Program (DGE-1650116, JTH), NIDCR of the National Institutes of Health (F32DE026683, TMJ), the National Institutes of Health (5-R01-CA193140, EL, BS, GD), The David and Lucile Packard Foundation (2013-39274, SKL), Eshelman Institute for Innovation (SKL), a Dissertation Completion Fellowship from The Graduate School at UNC-Chapel Hill (JTH), and startup funds from the Eshelman School of Pharmacy and Lineberger Comprehensive Cancer Center at UNC-Chapel Hill (SKL).

Competing interests TMJ has an equity interest in Dualogics LLC, a company aimed at commercializing bispecific antibodies.

Patient consent for publication Not required.

Ethics approval All tumor mouse model experiments were performed in accordance with UNC Animal Husbandry and Institutional Animal Care and Use Committee (IACUC) guidelines and were approved by UNC IACUC (Protocol #: 18–251).

Provenance and peer review Not commissioned; externally peer reviewed.

Data availability statement Data are available on reasonable request. All data relevant to the study are included in the article or uploaded as supplementary information.

Supplemental material This content has been supplied by the author(s). It has not been vetted by BMJ Publishing Group Limited (BMJ) and may not have been peer-reviewed. Any opinions or recommendations discussed are solely those of the author(s) and are not endorsed by BMJ. BMJ disclaims all liability and responsibility arising from any reliance placed on the content. Where the content includes any translated material, BMJ does not warrant the accuracy and reliability of the translations (including but not limited to local regulations, clinical guidelines, terminology, drug names and drug dosages), and is not responsible for any error and/or omissions arising from translation and adaptation or otherwise.

Open access This is an open access article distributed in accordance with the Creative Commons Attribution Non Commercial (CC BY-NC 4.0) license, which permits others to distribute, remix, adapt, build upon this work non-commercially, and license their derivative works on different terms, provided the original work is properly cited, appropriate credit is given, any changes made indicated, and the use is non-commercial. See http://creativecommons.org/licenses/by-nc/4.0/.

ORCID iD

Samuel K Lai http://orcid.org/0000-0003-4721-528X

REFERENCES

1 June CH, O'Connor RS, Kawalekar OU, *et al*. Car T cell immunotherapy for human cancer. *Science* 2018;359:1361–5.
2 Maude SL, Frey N, Shaw PA, *et al*. Chimeric antigen receptor T cells for sustained remissions in leukemia. *N Engl J Med* 2014;371:1507–17.
3 Leick MB, Maus MV, Frigault MJ. Clinical perspective: treatment of aggressive B cell lymphomas with FDA-approved CAR-T cell therapies. *Mol Ther* 2021;29:433–41.
4 Gomes-Silva D, Ramos CA. Cancer immunotherapy using CAR-T cells: from the research bench to the assembly line. *Biotechnol J* 2018;13:1700097–8.
5 Levine BL, Miskin J, Wonnacott K, *et al*. Global manufacturing of CAR T cell therapy. *Mol Ther Methods Clin Dev* 2017;4:92–101.
6 Vormittag P, Gunn R, Ghorashian S, *et al*. A guide to manufacturing CAR T cell therapies. *Curr Opin Biotechnol* 2018;53:164–81.
7 Wang X, Rivière I. Clinical manufacturing of CAR T cells: Foundation of a promising therapy. *Mol Ther Oncolytics* 2016;3:16015.
8 Papathanasiou MM, Stamatis C, Lakelin M, *et al*. Autologous CAR T-cell therapies supply chain: challenges and opportunities? *Cancer Gene Ther* 2020;27:799–809.
9 McLellan AD, Ali Hosseini Rad SM. Chimeric antigen receptor T cell persistence and memory cell formation. *Immunol Cell Biol* 2019;97:664–74.
10 Lim WA, June CH. The principles of engineering immune cells to treat cancer. *Cell* 2017;168:724–40.
11 Li Y, Kurlander RJ. Comparison of anti-CD3 and anti-CD28-coated beads with soluble anti-CD3 for expanding human T cells: differing impact on CD8 T cell phenotype and responsiveness to restimulation. *J Transl Med* 2010;8:104.
12 Gattinoni L, Klebanoff CA, Palmer DC, *et al*. Acquisition of full effector function in vitro paradoxically impairs the in vivo antitumor

J Immunother Cancer: first published as 10.1136/jitc-2021-002737 on 12 September 2021. Downloaded from http://jitc.bmj.com/ on April 18, 2024 by guest. Protected by copyright.

efficacy of adoptively transferred CD8+ T cells. *J Clin Invest* 2005;115:1616–26.
13 Casado JG, DelaRosa O, Pawelec G, *et al*. Correlation of effector function with phenotype and cell division after in vitro differentiation of naive MART-1-specific CD8+ T cells. *Int Immunol* 2009;21:53–62.
14 Klebanoff CA, Scott CD, Leonardi AJ, *et al*. Memory T cell-driven differentiation of naive cells impairs adoptive immunotherapy. *J Clin Invest* 2016;126:318–34.
15 Petersen CT, Hassan M, Morris AB, *et al*. Improving T-cell expansion and function for adoptive T-cell therapy using ex vivo treatment with PI3Kδ inhibitors and VIP antagonists. *Blood Adv* 2018;2:210–23.
16 Hartmann J, Schüßler-Lenz M, Bondanza A, *et al*. Clinical development of CAR T cells-challenges and opportunities in translating innovative treatment concepts. *EMBO Mol Med* 2017;9:1183–97.
17 Milone MC, O'Doherty U. Clinical use of lentiviral vectors. *Leukemia* 2018;32:1529–41.
18 Bouard D, Alazard-Dany D, Cosset F-L. Viral vectors: from virology to transgene expression. *Br J Pharmacol* 2009;157:153–65.
19 Joglekar AV, Sandoval S. Pseudotyped lentiviral vectors: one vector, many Guises. *Hum Gene Ther Methods* 2017;28:291–301.
20 Cronin J, Zhang X-Y, Reiser J. Altering the tropism of lentiviral vectors through pseudotyping. *Curr Gene Ther* 2005;5:387–98.
21 Buchholz CJ, Friedel T, Büning H. Surface-Engineered viral vectors for selective and cell type-specific gene delivery. *Trends Biotechnol* 2015;33:777–90.
22 Frank AM, Buchholz CJ. Surface-Engineered lentiviral vectors for selective gene transfer into subtypes of lymphocytes. *Mol Ther Methods Clin Dev* 2019;12:19–31.
23 Funke S, Maisner A, Mühlebach MD, *et al*. Targeted cell entry of lentiviral vectors. *Mol Ther* 2008;16:1427–36.
24 Zhou Q, Schneider IC, Gallet M, *et al*. Resting lymphocyte transduction with measles virus glycoprotein pseudotyped lentiviral vectors relies on CD46 and SLAM. *Virology* 2011;413:149–52.
25 Zhou Q, Uhlig KM, Muth A, *et al*. Exclusive transduction of human CD4+ T cells upon systemic delivery of CD4-Targeted lentiviral vectors. *J Immunol* 2015;195:2493–501.
26 Bender RR, Muth A, Schneider IC, *et al*. Receptor-Targeted Nipah virus glycoproteins improve cell-type selective gene delivery and reveal a preference for membrane-proximal cell attachment. *PLoS Pathog* 2016;12:e1005641.
27 Pfeiffer A, Thalheimer FB, Hartmann S, *et al*. *In vivo* generation of human CD19-CAR T cells results in B-cell depletion and signs of cytokine release syndrome. *EMBO Mol Med* 2018;10:e9158.
28 Agarwal S, Weidner T, Thalheimer FB, *et al*. *In vivo* generated human CAR T cells eradicate tumor cells. *Oncoimmunology* 2019;8:e1671761.
29 Jamali A, Kapitza L, Schaser T, *et al*. Highly efficient and selective CAR-Gene transfer using CD4- and CD8-Targeted lentiviral vectors. *Mol Ther Methods Clin Dev* 2019;13:371–9.
30 Agarwal S, Hanauer JDS, Frank AM, *et al*. In Vivo Generation of CAR T Cells Selectively in Human CD4$^+$ Lymphocytes. *Mol Ther* 2020;28:1783–94.
31 Frank AM, Braun AH, Scheib L, *et al*. Combining T-cell-specific activation and in vivo gene delivery through CD3-targeted lentiviral vectors. *Blood Adv* 2020;4:5702–15.
32 Morizono K, Bristol G, XieYM, *et al*. Antibody-Directed targeting of retroviral vectors via cell surface antigens. *J Virol* 2001;75:8016–20.
33 Morizono K, Xie Y, Ringpis G-E, *et al*. Lentiviral vector retargeting to P-glycoprotein on metastatic melanoma through intravenous injection. *Nat Med* 2005;11:346–52.
34 Pariente N, Morizono K, Virk MS, *et al*. A novel dual-targeted lentiviral vector leads to specific transduction of prostate cancer bone metastases in vivo after systemic administration. *Mol Ther* 2007;15:1973–81.
35 Morizono K, Ringpis G-E, Pariente N, *et al*. Transient low pH treatment enhances infection of lentiviral vector pseudotypes with a targeting Sindbis envelope. *Virology* 2006;355:71–81.
36 Liang M, Morizono K, Pariente N, *et al*. Targeted transduction via CD4 by a lentiviral vector uses a clathrin-mediated entry pathway. *J Virol* 2009;83:13026–31.
37 Morizono K, Xie Y, Helguera G, *et al*. A versatile targeting system with lentiviral vectors bearing the biotin-adaptor peptide. *J Gene Med* 2009;11:655–63.
38 Morizono K, Pariente N, Xie Y, *et al*. Redirecting lentiviral vectors by insertion of integrin-tageting peptides into envelope proteins. *J Gene Med* 2009;11:549–58.
39 Situ K, Chua BA, Bae SY, *et al*. Versatile targeting system for lentiviral vectors involving biotinylated targeting molecules. *Virology* 2018;525:170–81.
40 Kasaraneni N, Chamoun-Emanuelli AM, Wright G, *et al*. Retargeting lentiviruses via SpyCatcher-SpyTag chemistry for gene delivery into specific cell types. *mBio* 2017;8:e01860–17.
41 Kasaraneni N, Chamoun-Emanuelli AM, Wright GA, *et al*. A simple strategy for retargeting lentiviral vectors to desired cell types via a disulfide-bond-forming protein-peptide pair. *Sci Rep* 2018;8:1–9.
42 Ziegler L, Yang L, Joo Kil, *et al*. Targeting lentiviral vectors to antigen-specific immunoglobulins. *Hum Gene Ther* 2008;19:861–72.
43 Froelich S, Ziegler L, Stroup K, *et al*. Targeted gene delivery to CD117-expressing cells in vivo with lentiviral vectors co-displaying stem cell factor and a fusogenic molecule. *Biotechnol Bioeng* 2009;104:206–15.
44 Yang L, Yang H, Rideout K, *et al*. Engineered lentivector targeting of dendritic cells for in vivo immunization. *Nat Biotechnol* 2008;26:326–34.
45 Yang H, Joo K-I, Ziegler L, *et al*. Cell type-specific targeting with surface-engineered lentiviral vectors co-displaying OKT3 antibody and fusogenic molecule. *Pharm Res* 2009;26:1432–45.
46 Lei Y, Joo K-I, Wang P. Engineering fusogenic molecules to achieve targeted transduction of enveloped lentiviral vectors. *J Biol Eng* 2009;3:8.
47 Frankel TL, Burns WR, Peng PD, *et al*. Both CD4 and CD8 T cells mediate equally effective in vivo tumor treatment when engineered with a highly avid TCR targeting tyrosinase. *J Immunol* 2010;184:5988–98.
48 Mastaglio S, Genovese P, Magnani Z, *et al*. Ny-Eso-1 TCR single edited stem and central memory T cells to treat multiple myeloma without graft-versus-host disease. *Blood* 2017;130:606–18.
49 Landoni E, Smith CC, Fucá G, *et al*. A high-avidity T-cell receptor redirects natural killer T-cell specificity and outcompetes the endogenous invariant T-cell receptor. *Cancer Immunol Res* 2020;8:57–69.
50 Lewis SM, Wu X, Pustilnik A, *et al*. Generation of bispecific IgG antibodies by structure-based design of an orthogonal Fab interface. *Nat Biotechnol* 2014;32:191–8.
51 Klein C, Sustmann C, Thomas M, *et al*. Progress in overcoming the chain association issue in bispecific heterodimeric IgG antibodies. *MAbs* 2012;4:653–63.
52 Parker CL, Jacobs TM, Huckaby JT, *et al*. Efficient and highly specific gene transfer using mutated lentiviral vectors redirected with bispecific antibodies. *mBio* 2020;11:1–12.
53 Frecha C, Costa C, Nègre D, *et al*. Stable transduction of quiescent T cells without induction of cycle progression by a novel lentiviral vector pseudotyped with measles virus glycoproteins. *Blood* 2008;112:4843–52.
54 Smith TT, Stephan SB, Moffett HF, *et al*. In situ programming of leukaemia-specific T cells using synthetic DNA nanocarriers. *Nat Nanotechnol* 2017;12:813–20.

J Immunother Cancer: first published as 10.1136/jitc-2021-002737 on 12 September 2021. Downloaded from http://jitc.bmj.com/ on April 18, 2024 by guest. Protected by copyright.

Bispecific binder redirected lentiviral vector enables *in vivo* engineering of CAR-T cells

Authors: Justin T. Huckaby[†,1], Elisa Landoni[†,2], Timothy M. Jacobs[3], Barbara Savoldo[2,4], Gianpietro Dotti[2,5], and Samuel K. Lai[*,1,3,5]

Affiliations:
[1]UNC/NCSU Joint Department of Biomedical Engineering
University of North Carolina at Chapel Hill
Chapel Hill, NC, 27599, USA.

[2]Lineberger Comprehensive Cancer Center
University of North Carolina at Chapel Hill
Chapel Hill, NC, 27599, USA.

[3]Divison of Pharmacoengineering and Molecular Pharmaceutics
University of North Carolina at Chapel Hill
Chapel Hill, NC, 27599, USA.

[4]Department of Pediatrics
University of North Carolina at Chapel Hill
Chapel Hill, NC, 27599, USA.

[5]Department of Microbiology and Immunology
University of North Carolina at Chapel Hill
Chapel Hill, NC, 27599, USA.

[*]To whom correspondence should be addressed: lai@unc.edu

[†]Co-first authors.

Huckaby JT, *et al. J Immunother Cancer* 2021; 9:e002737. doi: 10.1136/jitc-2021-002737

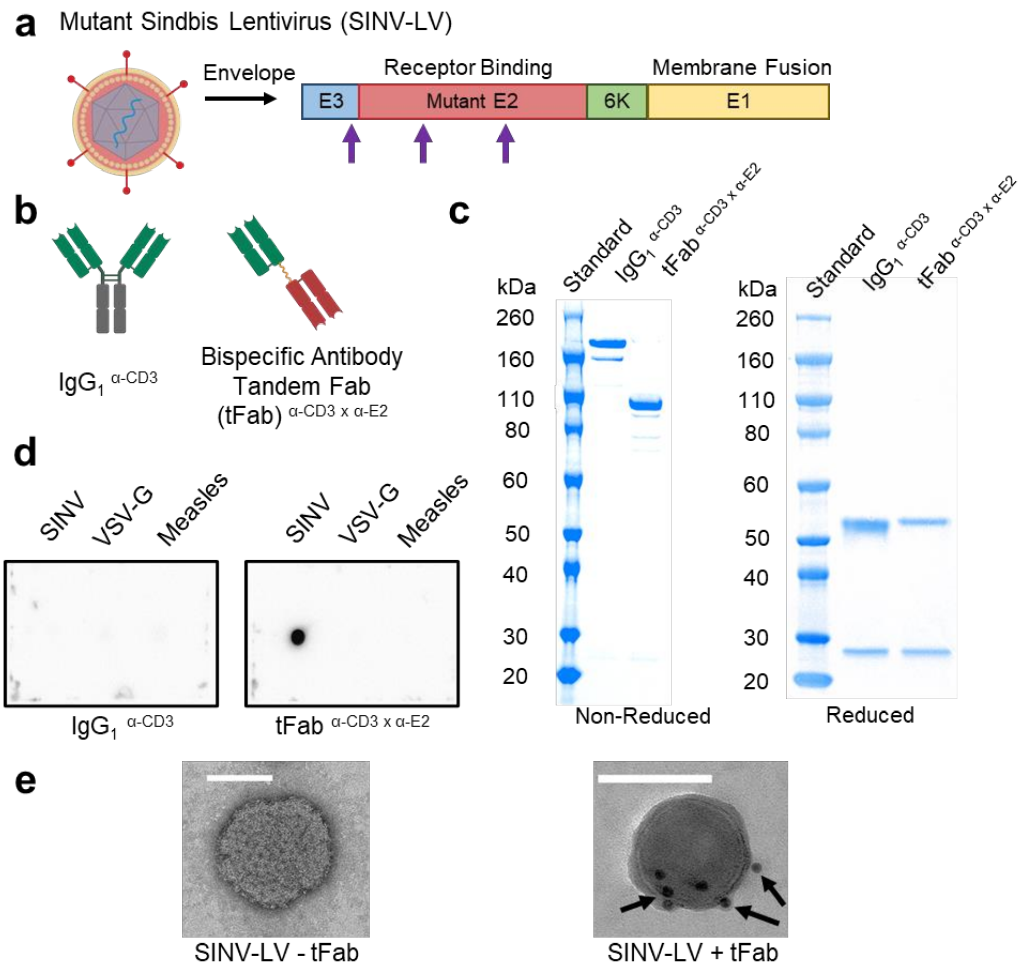

Figure S1: Characterization of mutant Sindbis lentivirus (SINV-LV) and bispecific antibody binder (tFab). a) Schematic representation of mutant Sindbis (SINV) envelope glycoproteins (E1 and E2) with purple arrows to denote mutations that ablate native receptor binding capabilities of the E2 domain. Mutations of the Sindbis envelope glycoprotein included: (i) deletion of residues 61-64 in the E3 leader sequence and (ii) SLKQ68-71AAAA and KE159-160AA in the E2 glycoprotein domain. The E1 domain is responsible for pH-dependent membrane fusion. E1 and E2 heterodimerize together to form trimeric spikes on the viral surface. **b)** Schematic representation of control anti-CD3 IgG (left panel) and anti-CD3 x anti-E2 bispecific antibody (tFab) (right panel). **c)** Non-reduced (left panel) and reduced (right panel) SDS-PAGE with Coomassie blue protein staining showing molecular weight and purity of control IgG and bispecific tFab. **d)** tFab binds specifically to SINV enveloped lentivirus and does not bind non-specifically to other common lentiviral pseudotypes (VSV-G and Measles Virus) as demonstrated by immunodot blotting. α-CD3 IgG negative control displays no binding to any of the three lentiviral pseudotypes tested. **e)** Transmission electron microscopy (TEM) images of SINV-LV without addition of tFab (left panel) and with addition of tFab (right panel) to confirm

binding and presence of tFab on targeted lentiviral surface (arrows) Scale bars (white; upper left) represent 100 nm.

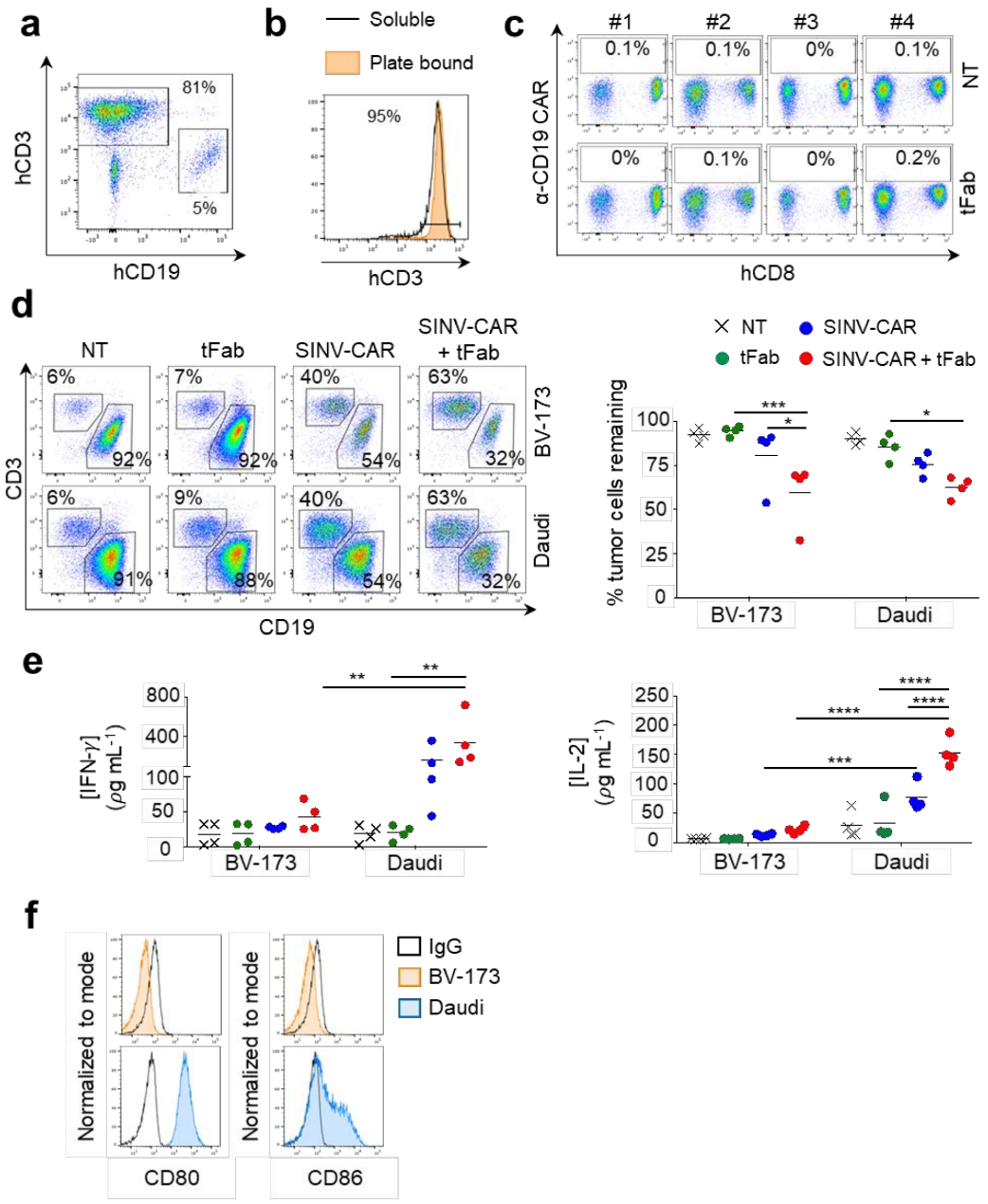

Figure S2: T cells transduced with SINV-CAR in combination with tFab express functional CD19.CAR and eliminate tumor B cells *in vitro*. a) Representative flow plots showing the composition of B cells and T cells in human PBMCs 2 days after isolation. **b)** CD3 expression in PBMCs detected with a commercial antibody after 24 hours of rest in complete medium following prior activation with either soluble or plate-bound anti-CD3 and anti-CD28 antibodies. **c)** Flow cytometry plots showing negative CAR expression in primary T cell transduction studies without SINV-CAR, including non-transduced (NT) and tFab alone control samples not included

in Figure 2b. **d)** Representative flow plots (left panel) and quantification summary (right panel) of residual tumor cells remaining in cocultures with NT, tFab, SINV-CAR, or SINV-CAR plus tFab treated T cells (E:T = 1:1) for 4 or 5 days (BV-173 and Daudi, respectively). All cells were collected and stained with CD3 and CD19 mAbs to identify T cells and tumor cells, respectively, by flow cytometry (n = 4, mean shown). *, P=0.0350 SINV-CAR plus tFab vs SINV-CAR; *, P=0.0175 SINV-CAR plus tFab vs tFab; **P=0.0003, two-way ANOVA. **e)** Quantification of IFNγ (left panel) and IL-2 (right panel) cytokine production in supernatant collected after 48 hours of co-culturing NT, tFab, SINV-CAR, or SINV-CAR plus tFab treated T cells with tumor cell lines (E:T = 1:1) (n = 4, mean shown). **P<0.0021, ***P=0.0002****P<0.0001, two-way ANOVA. **f)** Flow plots showing the CD80 and CD86 expression in BV-173 and Daudi cell lines.

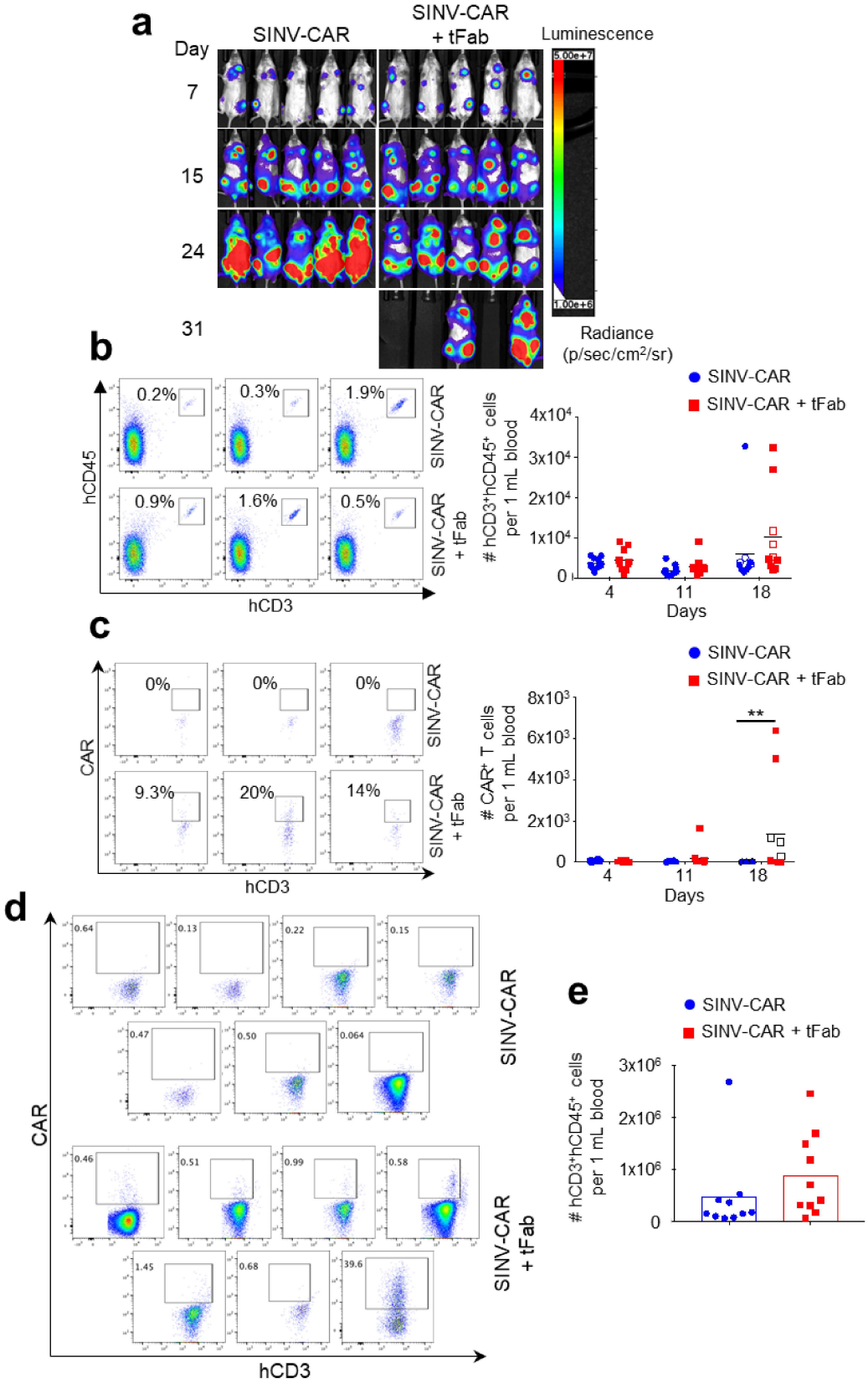
a
SINV-CAR
SINV-CAR + tFab
Luminescence
Day
7
15
24
31
Radiance (p/sec/cm²/sr)
b
hCD45
hCD3
SINV-CAR
SINV-CAR + tFab
0.2%
0.3%
1.9%
0.9%
1.6%
0.5%
hCD3⁺hCD45⁺ cells per 1 mL blood
Days
c
CAR
0%
9.3%
20%
14%
CAR⁺ T cells per 1 mL blood
**
d
0.64
0.13
0.22
0.15
0.47
0.50
0.064
0.46
0.51
0.99
0.58
1.45
0.68
39.6
e
hCD3⁺hCD45⁺ cells per 1 mL blood

Figure S3: Absolute numbers of T cells detected from weekly bleeds in mice of *in vivo* tumor model. a) Representative tumor bioluminescence (BLI) (color scale: min = 1 x 10^6; max = 5 x 10^7) for mice treated according to scheme from Figure 3a. **b)** Representative flow plots (left panel) of the percentage of $CD3^+CD45^+$ human T cells in the peripheral blood at day 18. Quantification summary (right panel) of the number of $CD3^+CD45^+$ human T cells in the peripheral blood 4, 11, and 18 days after PBMCs injection (n = 10 each condition, mean shown). Empty symbols denote the flow plots shown to the left. **c)** Representative flow plots (left panel) of the percentage of human CAR-T cells (gated on $CD3^+CD45^+$) in the peripheral blood at day 18. Quantification summary (right panel) of the number of human CAR-T cells (gated on $CD3^+CD45^+$) in the peripheral blood 4, 11 and 18 days after PBMCs injection (n = 10 each condition, mean shown). Empty symbols denote the flow plots shown to the left. **, P=0.0073, two-way ANOVA. **d)** Flow plots of CAR-T cells (gated on $CD3^+CD45^+$) in the peripheral blood at the time of euthanasia. **e)** Quantification summary of the number of $hCD3^+hCD45^+$ T cells in the peripheral blood at the time of euthanasia (n = 10 each condition, mean shown).

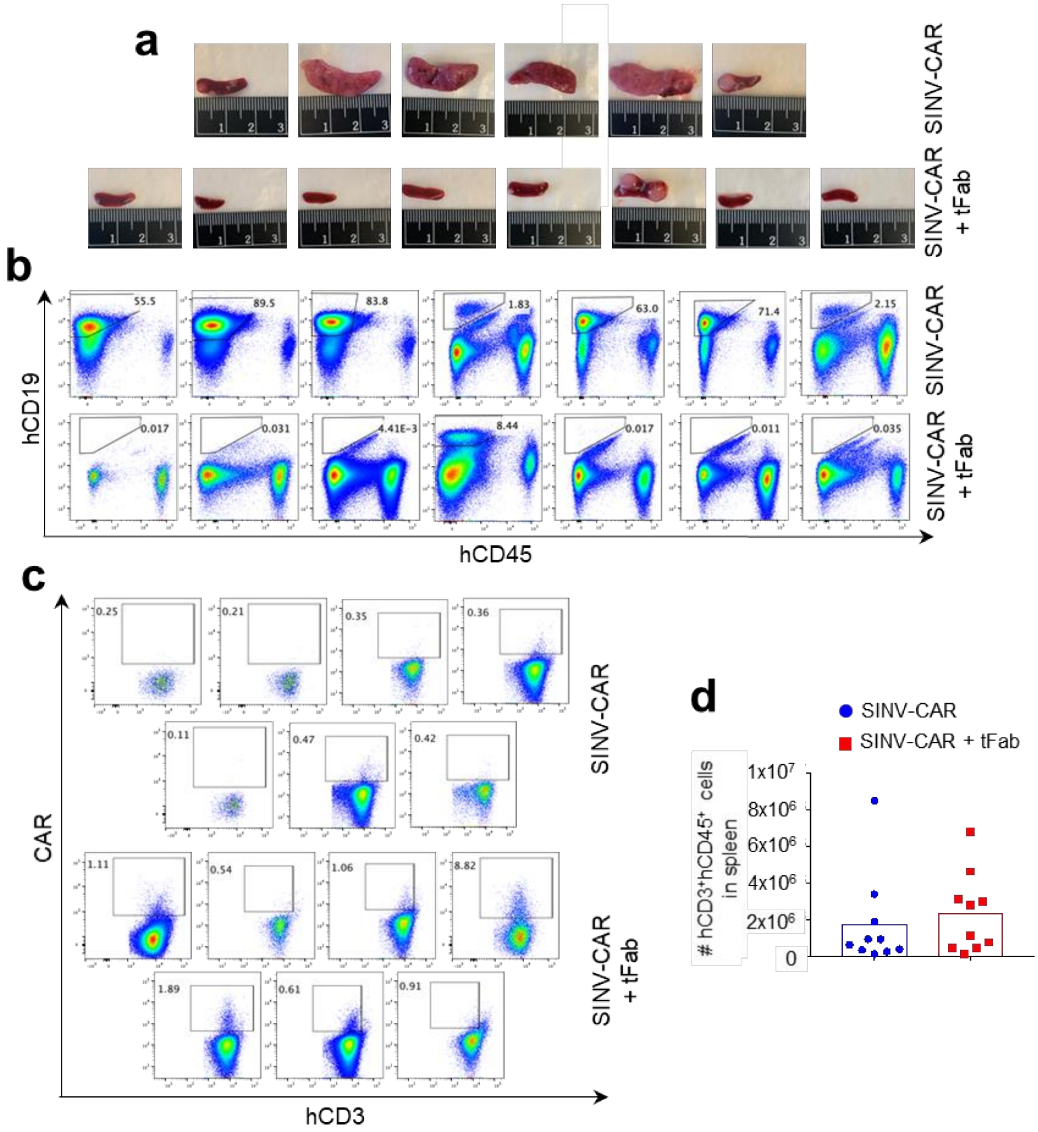

Figure S4: Absolute numbers of T cells detected from sacrifice in mice of *in vivo* tumor model. a) Mice engrafted with FFLuc BV-173 tumor cells and treated with either SINV-CAR alone or SINV-CAR plus tFab were euthanized, shown are the images of the spleens. **b)** Flow plots of human CAR-T cells (gated on $CD3^+CD45^+$) in the spleen at the time of euthanasia. **c)** Flow plots of human CAR-T cells (gated on $CD3^+CD45^+$) in the spleen at the time of euthanasia. **d)** Quantification summary of the number of $hCD3^+hCD45^+$ T cells in the spleen at the time of euthanasia (n = 10 each condition, mean shown).

Supplementary Methods

Immunophenotyping

T cells were stained with Abs against CD3 (APC-H7, clone SK7), CD8 (Alexa Fluor 700, clone RPA-T8) and CD45 (APC, clone 2D1) from BD Biosciences. Tumor cells were stained with Ab against CD19 (FITC, clone SJ25C1) from BD Biosciences. The expression of the anti-CD19 CAR was assessed using specific anti-idyotipic Ab, followed by the staining with a secondary rat anti-Mouse Ab (PE, clone X56) from BD Biosciences. Data acquisition was performed on BD LSRFortessa or Canto II flow cytometer using the BD FACS-Diva software or on a MACSQuant (Miltenyi Biotec). Data analyses was performed with the FlowJo software (Version 9 or 10).

Lentiviral vector design, production, and titration

Mutant Sindbis pseudotyped lentiviruses (SINV-LV) were generated via four plasmid transfection in 293T packaging cells. The mutant Sindbis envelope plasmid was constructed by cloning the Sindbis virus glycoprotein insert from plasmid 2.2 (Addgene plasmid no. 34885) [1] into an expression vector plasmid backbone under the CAG promoter. The ZZ domains of Protein A were removed from the mutant E2 domain of the new mammalian expression plasmid via Gibson Assembly cloning. Mutations of the Sindbis envelope glycoprotein included: (i) deletion of residues 61-64 in the E3 leader sequence and (ii) SLKQ68-71AAAA and KE159-160AA in the E2 glycoprotein domain. Negative control envelope plasmids for antibody binding specificity studies were kind gifts of Bob Weinberg (pCMV-VSV-G, Addgene plasmid no. 8454) [2] and Jakob Reiser (pCG-HcΔ18, Addgene plasmid no. 84817). To generate functional pseudotyped LV vectors with measles virus glycoproteins, Jakob Reiser also provided the sequence for cloning the measles virus fusion (F) protein envelope plasmid (pCG-FcΔ30) [3].

The pLL3.7 transfer plasmid (Addgene plasmid no. 11795) was a gift from Luk Parijs [4] and used as the transgene cassette for expressing eGFP as a reporter of transduction in SINV-GFP. Using NotI and BspEI in a restriction enzyme double digest, we generated a new transfer plasmid, pLL CD19 CAR, from the pLL3.7 plasmid backbone for producing SINV-CAR. The new gene cassette for pLL CD19 CAR consisted of an EF-1α internal promoter, anti-CD19 scFv, CD8 flexible hinge domain, CD8 transmembrane domain, CD28 costimulatory endodomain, CD3ζ chain, and WPRE post-transcriptional regulatory element all flanked by the original LTRs of the pLL3.7 plasmid backbone. Third generation lentiviral packaging plasmids pMDLg/pRRE (Addgene plasmid no. 12251) and pRSV-Rev (Addgene plasmid no. 12253) were gifts of Didier Trono [5]. LV were produced via transient transfection of LV-MAX cells according to manufacturer protocols for the LV-MAX lentiviral production system kit (Gibco). Briefly, 1.2 x 10^8 viable cells were seeded in a vented shaker flask for a final production volume of 30 mL. A 3:2 ratio of packaging plasmids (envelope, gag/pol, and rev) to transfer plasmid was combined with LV-MAX Transfection Reagent in serum-free medium and subsequently added to cells in shaker flask after 10 minutes of incubation. At ~ 48 hours following transfection, cells were collected from suspension culture along with their medium and centrifuged at 1,300 x g for 15 mins to pellet cells. Supernatant containing LV vectors was harvested and filtered through a 0.45 μm low protein binding filter to further remove cell debris. Filtered supernatant was added carefully dropwise to a sucrose cushion (25% w/v sucrose in HEPES-NaCl buffer) and subjected to ultracentrifugation at 36,000 rpm for 2.5 hrs at 4˚C. Following ultracentrifugation, supernatant and sucrose cushion were carefully aspirated leaving LV pellet at bottom center of tubes. LV pellets were resuspended overnight at 4˚C with 10% w/v sucrose in HEPES-NaCl buffer, aliquoted, and frozen at -80C for long-term storage. *In vivo* grade LV was prepared by the Duke

University Viral Vector Core (Boris Kantor Lab) using calcium phosphate-based transfection of adherent HEK-293T cells and subsequent double-sucrose gradient purification [6]. All LV were titered immediately after thawing a fresh aliquot on ice using a qPCR lentiviral titration kit according to manufacturer protocols (Applied Biological Materials Inc., Cat # LV900).

Bispecific antibody binder construction, expression, and characterization

Heavy and light chain antibody constructs were generated on separate mammalian expression vectors, each with the same backbone and CAG promoter sequence. Twist Bioscience performed the molecular cloning of antibody gene constructs for mammalian expression. Following an albumin signal peptide for protein secretion, the bispecific antibody (BsAb) tandem Fab (tFab) heavy chain construct consisted of a murine anti-Sindbis E2 variable heavy domain (V_H) and human IgG_1 constant heavy 1 domain (C_{H1}) covalently linked with a humanized anti-CD3 V_H and human IgG_1 C_{H1} by a flexible glycine-serine peptide linker $(G_4S)_6$. The C-terminus of this V_H-C_{H1}-Linker-V_H-C_{H1} bispecific heavy chain construct contained an 8x polyhistidine tag for purification purposes. A separate construct was designed for each of the two different light chains of the tFab. The anti-Sindbis E2 light chain consisted of a variable light domain and human constant lambda light chain domain (V_L-C_λ), while the anti-CD3 light chain consisted of a variable light domain and human constant kappa light chain domain (V_L-C_κ). The murine anti-Sindbis E2 V_H/V_L sequences were kindly provided by Diane Griffin (Johns Hopkins University; unpublished results), and the anti-CD3 V_H/V_L sequences were publicly available from a humanized version of the mAb clone UCHT1 [7]. To generate the bispecific tFab ($Fab^{\alpha\text{-}E2}$ – Linker – $Fab^{\alpha\text{-}CD3}$), separate orthogonal amino acid mutation sets were incorporated into the separate anti-E2 and anti-CD3 Fab domains [8]. These orthogonal mutation sets provided high-

fidelity pairing of antibody heavy and light chains for correct assembly of desired BsAb molecule. This OrthoMab technology to generate high-fidelity BsAbs was licensed through a partnership between Dualogics and UNC-CH. A humanized anti-CD3 IgG_1 mAb ($IgG_1^{\alpha\text{-}CD3}$) was also generated with the same set of orthogonal mutations from the tFab's anti-CD3 portion and used as a control molecule for *in vitro* experimentation.

Plasmids encoding the antibody heavy and light chains were co-transfected at equimolar ratios into Expi293F mammalian cells using the ExpiFectamine 293 transfection kit based on manufacturer protocols (Gibco). tFab required co-transfection of three separate plasmids at equimolar ratios (heavy chain plasmid, anti-E2 light chain plasmid, and anti-CD3 light chain plasmid), while $IgG_1^{\alpha\text{-}CD3}$ only required co-transfection of two separate plasmids at equimolar ratios (anti-CD3 heavy chain plasmid including an IgG_1 Fc and anti-CD3 light chain plasmid). After ~5 days of recombinant protein expression, suspension cells were pelleted by centrifugation at 8,000 x g, and the supernatant containing expressed antibodies was harvested and filtered through a 0.2 μm PES filter. tFab $^{\alpha\text{-}CD3 \times \alpha\text{-}E2}$ was purified from cell culture supernatant via immobilized metal affinity chromatography (IMAC) using Ni-NTA agarose (Qiagen). $IgG_1^{\alpha\text{-}CD3}$ was purified from cell culture supernatant via affinity chromatography using protein A plus agarose (ThermoFisher Scientific). Purified proteins were simultaneously concentrated and buffer exchanged into PBS using ultrafiltration (MWCO 30 K, Amicon Ultra). Antibody concentration was determined by spectrophotometry measurements using calculated protein extinction coefficients (A280 NanoDrop^{TM} One/One^{C}). The size and purity of purified antibodies were assessed by sodium dodecyl sulfate polyacrylamide gel electrophoresis (SDS-PAGE), and protein bands were detected with Coomassie stain (Imperial Protein Stain, Thermo Scientific).

Antibody binding assays

Indirect enzyme-linked immunosorbent assay (ELISA) was used to characterize and compare binding affinities of purified antibodies to both target antigens: human CD3ε and mutant Sindbis E2 glycoprotein. Briefly, either human CD3ε protein (Novus Biologicals, Cat # NBP2-22752) or SINV-LV particles, purified from in-house recombinant production (see above), were coated as antigen onto high binding, half-area, clear 96-well plates (Corning Costar, Cat # 3690) overnight at 4˚C. Human CD3ε protein was diluted to 1 μg mL^{-1} in carb-bicarb buffer (pH 9.6, Sigma C3041) for overnight coating, while purified SINV-LV stocks were diluted 100-fold in the same carb-bicarb buffer for overnight coating. The next morning, plates were washed 5x with PBS-0.05% Tween (PBST) and subsequently blocked for 1-2 hours at room temperature with 5% w/v non-fat milk in PBST. Purified antibody samples and controls were serially diluted in 1% w/v milk-PBST, spanning at least three orders of magnitude in concentration, and added to the blocked plates for 1-2 hour incubation at room temperature. Following 5x PBST washes of the plates, bound antibodies were detected using goat anti-human kappa light chain HRP conjugated secondary antibody (Sigma-Aldrich, Cat # A7164) at 1:1,000 dilution in 1% w/v milk-PBST for 1 hour incubation at room temperature. Following 5x PBST washes to remove unbound secondary detection antibody, 1-Step Ultra TMB-ELISA substrate solution (Thermo Scientific) was added for up to 10 mins to detect HRP activity. The enzymatic reaction was quenched by adding equal volume of 2 N sulfuric acid, and the color development was immediately determined by taking absorbance measurements at 450 nm (signal) and 570 nm (background) wavelengths using a SpectraMax M2 microplate reader (Molecule Devices).

Negative control wells, including antigen coated, blocked wells without primary antibody incubation and uncoated, blocked wells with primary antibody incubation, both revealed negligible signal development in the assay. Background subtracted absorbance values for each sample condition, run in triplicate, were imported into GraphPad Prism 8 software for calculating the binding affinity of each antibody titration curve and presented as equilibrium dissociation constants (K_D). A nonlinear curve fit with one site – specific binding was used to determine the K_D values.

To evaluate the specificity of tFab binding to mutant Sindbis glycoproteins, purified LVs, made from the same passage of LV-MAX packaging cells, with different envelopes (SINV, VSV-G, and Measles) were blotted directly onto a nitrocellulose membrane for dot blot immunoassay. Briefly, nitrocellulose membranes were blotted directly with 1 µL of purified LV samples of different envelope pseudotypes. Once samples were dry, the membranes were washed 5x with PBST before blocking the membranes for 1 hour at room temperature in 5% w/v milk-PBST with gentle agitation. $IgG_1^{\alpha\text{-}CD3}$ negative control or tFab $^{\alpha\text{-}CD3 \times \alpha\text{-}E2}$ were diluted separately to 3 µg mL^{-1} concentration in 1% w/v milk-PBST. The blocked membranes were transferred separately to these primary antibody solutions and incubated for 1 hour at room temperature with gentle agitation for antibody binding. After 5x washes with PBST, primary antibodies bound to the membranes were detected using goat anti-human kappa light chain HRP conjugated secondary antibody (Sigma-Aldrich, Cat # A7164) at 1:1,000 dilution in 1% w/v milk-PBST for 1 hour incubation at room temperature with gentle agitation. After 5x washes with PBST, the membranes were imaged together with identical exposure times using a ChemiDoc XRS+ imaging system (Bio-Rad). Chemiluminescent signal of secondary antibody binding was detected using Clarity Western ECL substrate (Bio-Rad, Cat # 1705061).

Transmission electron microscopy (TEM) of lentivirus

Purified SINV-LV was incubated on a glow discharged CF300Cu grid. Excess sample was wicked away from the grid and rinsed with washing buffer (1x PBS). The grid was blocked in 1% w/v BSA-PBS, rinsed with washing buffer, and incubated with tFab (10 μg mL^{-1}) at room temperature. Following another buffer rinse, secondary gold bead conjugated antibody (Abcam, Cat # ab39596) was incubated with the grid at a final stock dilution of 1:50 at room temperature. The grid was rinsed with washing buffer prior to addition of 4% PFA for fixation. Following a final buffer rinse, negative staining was performed. The grid was rinsed with DI water followed by addition of 1% uranyl acetate solution to the grid for 10 minutes. A final rinse with DI water was performed. The entire process took place in a 150 x 15 mm petri dish to prevent evaporation of solutions. Images were captured using an FEI Tecnai T12 transmission electron microscope at 120 kV.

References

1. Pariente N, Morizono K, Virk MS, Petrigliano FA, Reiter RE, Lieberman JR, et al. A novel dual-targeted lentiviral vector leads to specific transduction of prostate cancer bone metastases in vivo after systemic administration. Mol Ther. The American Society of Gene Therapy; 2007;15:1973–81.

2. Stewart SA, Dykxhoorn DM, Palliser D, Mizuno H, Yu EY, An DS, et al. Lentivirus-delivered stable gene silencing by RNAi in primary cells. RNA. 2003;9:493–501.

3. Marino MP, Panigaj M, Ou W, Manirarora J, Wei CH, Reiser J. A scalable method to concentrate lentiviral vectors pseudotyped with measles virus glycoproteins. Gene Ther. Nature Publishing Group; 2015;22:280–5.

4. Rubinson DA, Dillon CP, Kwiatkowski A V., Sievers C, Yang L, Kopinja J, et al. A lentivirus-based system to functionally silence genes in primary mammalian cells, stem cells and transgenic mice by RNA interference. Nat Genet. 2003;33:401–6.

5. Dull T, Zufferey R, Kelly M, Mandel RJ, Nguyen M, Trono D, et al. A Third-Generation Lentivirus Vector with a Conditional Packaging System. J Virol. 1998;72:8463–71.

6. Vijayraghavan S, Kantor B. A protocol for the production of integrase-deficient lentiviral vectors for CRISPR/Cas9-mediated gene knockout in dividing cells. J Vis Exp. 2017;130:1–8.

7. Shalaby MR, Shepard HM, Presta L, Rodrigues ML, Beverley PCL, Feldmann M, et al. Development of humanized bispecitic antibodies reactive with cytotoxic lymphocytes and tumor cells overexpressing the HER2 protooncogene. J Exp Med. 1992;175:217–25.

8. Lewis SM, Wu X, Pustilnik A, Sereno A, Huang F, Rick HL, et al. Generation of bispecific IgG antibodies by structure-based design of an orthogonal Fab interface. Nat Biotechnol. Nature Publishing Group; 2014;32:191–8.

Bispecific binder redirected lentiviral vector enables *in vivo* engineering of CAR-T cells

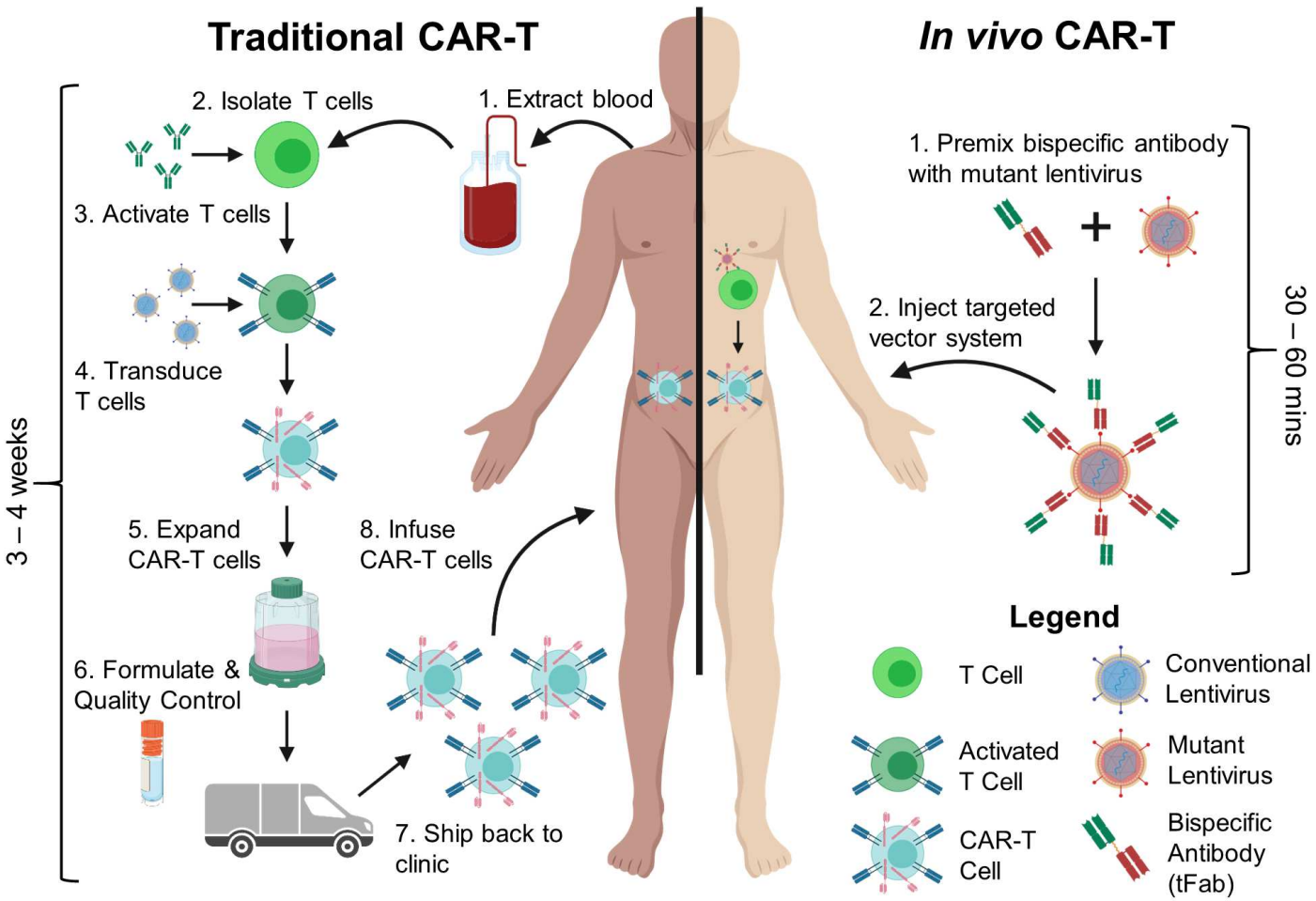

Authors

Justin T. Huckaby, Elisa Landoni, Timothy M. Jacobs, Barbara Savoldo, Gianpietro Dotti, Samuel K. Lai

Correspondence

lai@unc.edu

In Brief

A highly specific and efficient lentiviral gene delivery system, comprising a mutant envelope glycoprotein and bispecific antibody binder for redirection, generates CD19-specific CAR-T cells directly *in vivo* from a single injection and suppresses tumor growth to significantly extend the survival time of mice in an aggressive xenograft B cell tumor model.